ISCI, Volume *21*

Supplemental Information

Single-Cell RNA-seq Reveals Profound Alterations in Mechanosensitive Dorsal Root Ganglion Neurons with Vitamin E Deficiency

Carrie J. Finno, Janel Peterson, Mincheol Kang, Seojin Park, Matthew H. Bordbari, Blythe Durbin-Johnson, Matthew Settles, Maria C. Perez-Flores, Jeong H. Lee, and Ebenezer N. Yamoah

Supplemental Figures

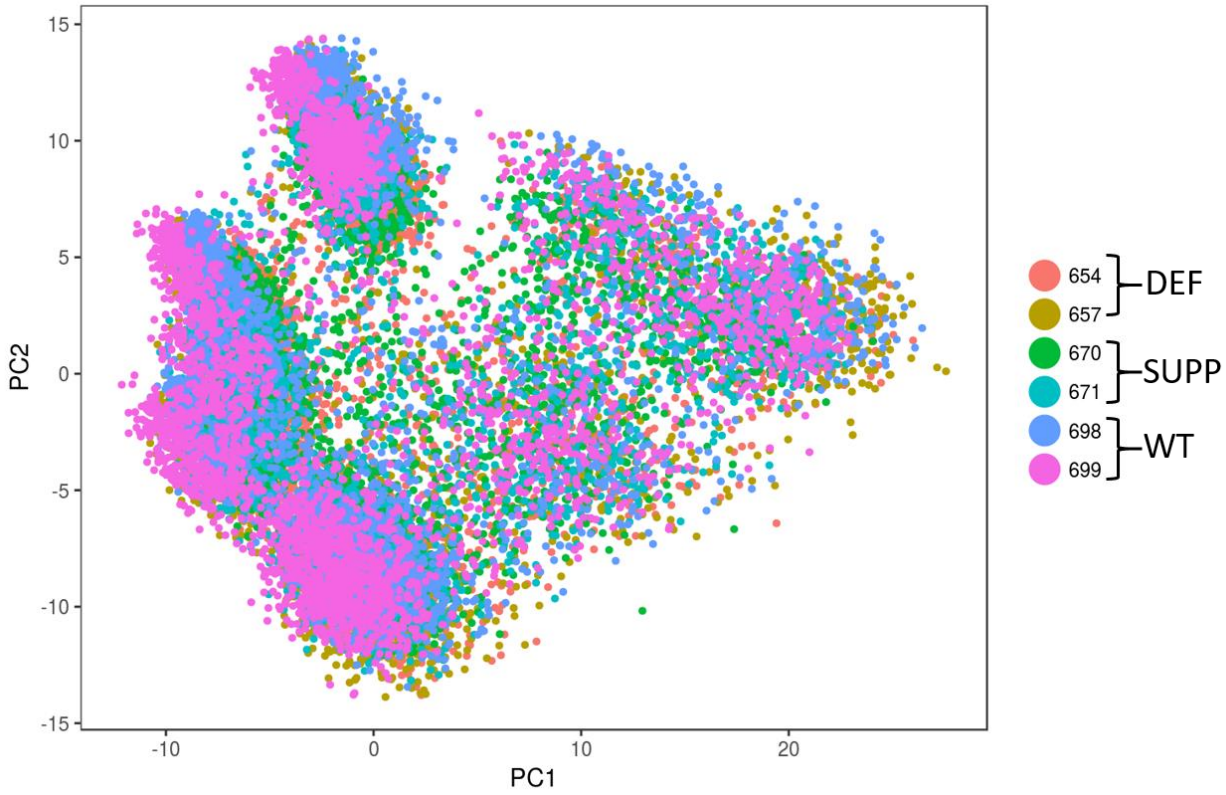

Figure S1, related to Figure 1A: Principal component analysis identified no difference in neuronal clustering between experimental groups.

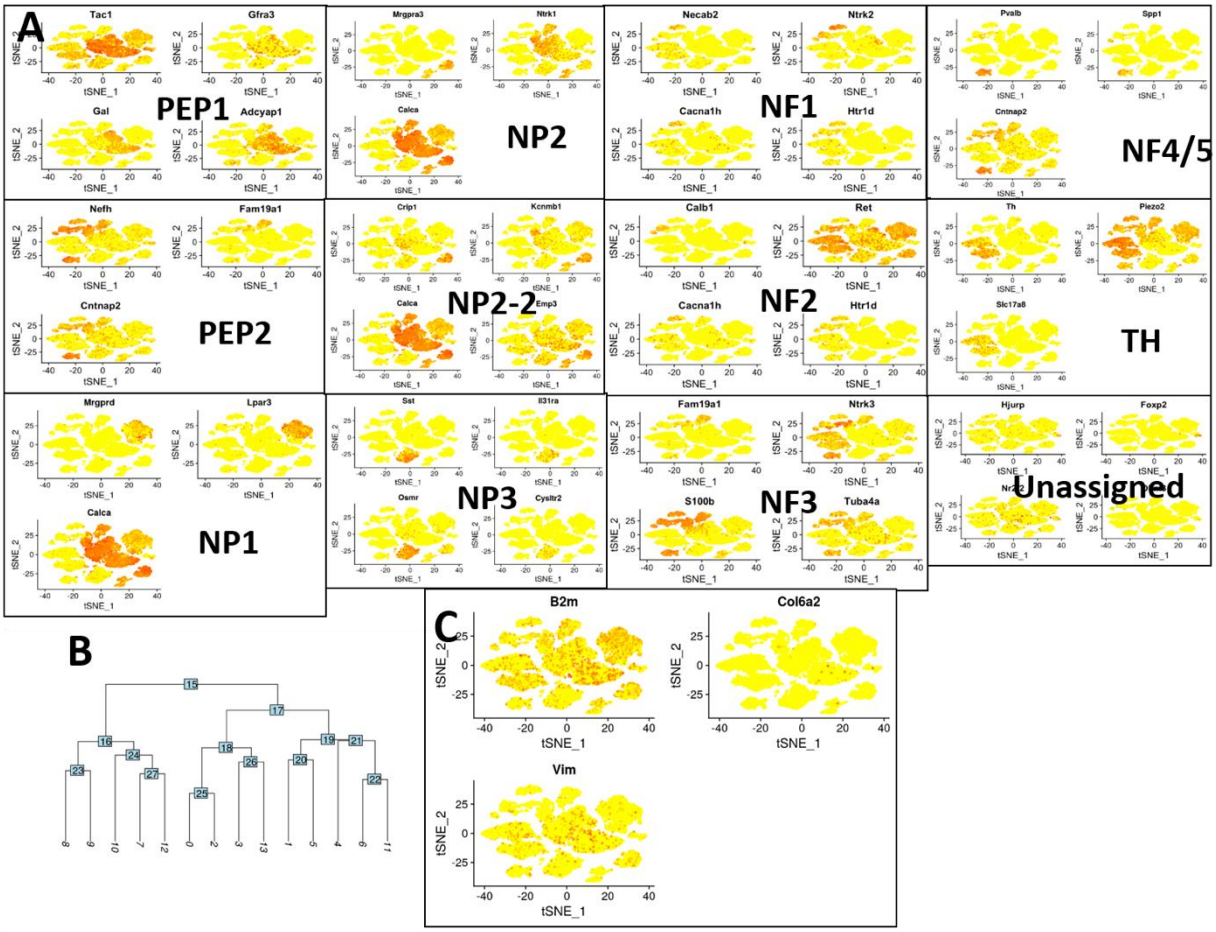

Figure S2, related to Figure 1A: (A) Classification of DRG subpopulations based on previously reported gene expression profiles (Li et al., 2016; Usoskin et al., 2015). NF=neurofilament, NP=non-peptidergic, PEP=peptidergic, TH=tyrosine hydroxylase, UNASSIGNED=unassigned cluster, n=2 mice per group with ~3,600 cells/mouse profiled. **(b)** Cluster dendogram used to determine subpopulations. Clusters 0 and 2 were merged into Cluster 0.2 based on shared peptidergic neuronal cell markers. **(C)** A distinct subpopulation of microglia cells, using previously identified transcriptional markers, was not identified in this dataset (Li et al., 2016; Usoskin et al., 2015).

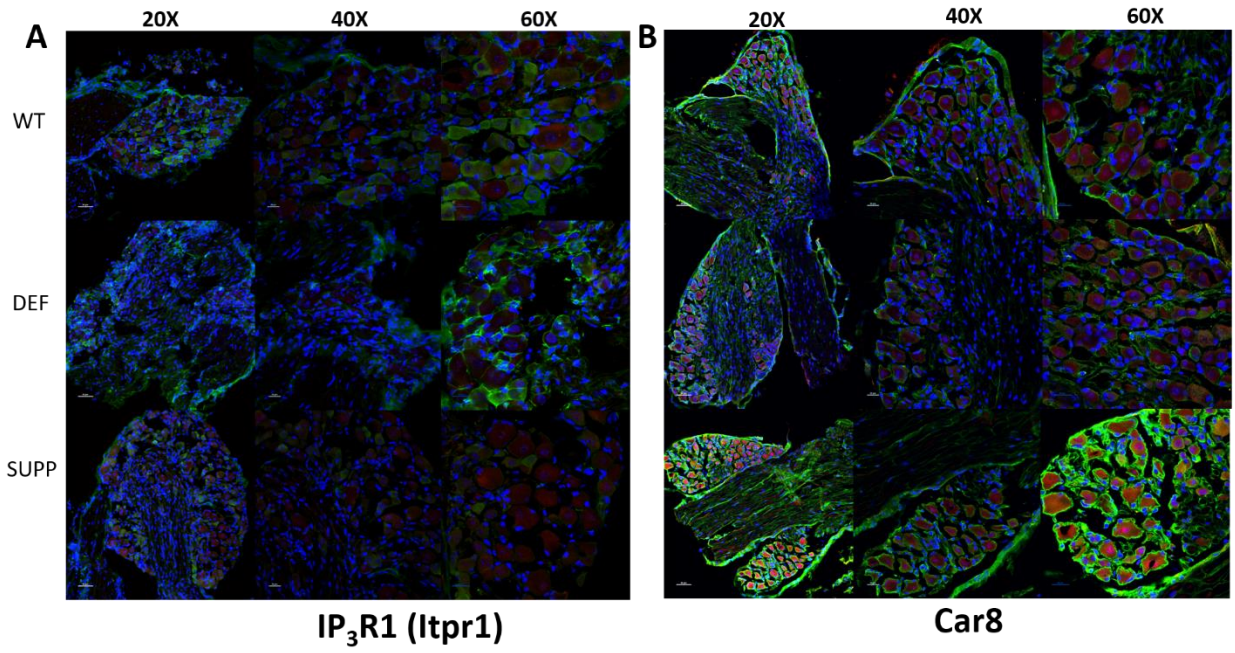

Figure S3, related to Fig. 1C: Triple-labeling identified decreased (A) IP_3R1 (Itpr1) and decreased (B) Car8 protein expression in tyrosine hydroxylase positive DRGN with vitE deficiency. Red: IP_3R1 (Itpr1) **(A)** or Car8 **(B)**; Green: Th, Blue: DAPI nuclei. Fluorescent immunohistochemistry from 4-month WT, DEF, and SUPP mice. 20x=50 μm, 40x=20 μm, 60x=20 μm

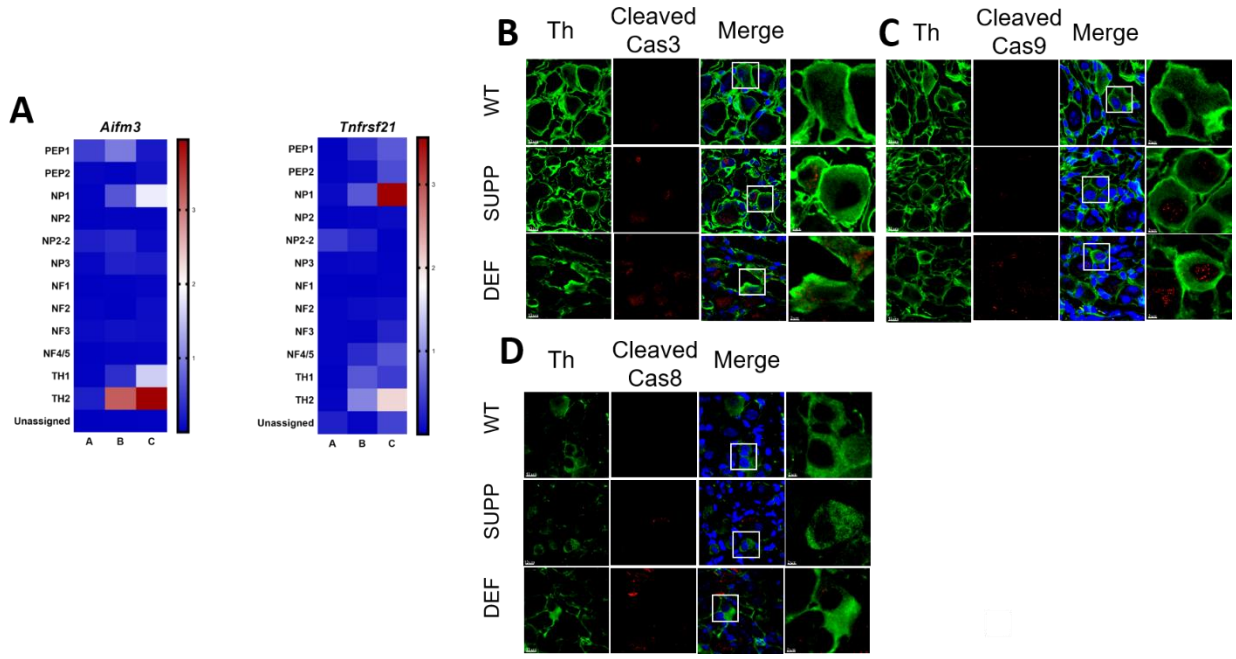

Figure S4, related to Fig. 7: Apoptosis of TH+ DRGNs with vitE deficiency. (A) Heat maps, plotted by $-\log P_{adjusted}$, comparing the degree of upregulation for apoptotic transcripts in DRGN subpopulations with α-TOH deficiency, with the most significantly upregulation in the Th2 subpopulation. Contrast A= SUPP vs. WT, contrast B= WT vs. DEF, contrast C= SUPP vs. DEF. *Aifm3*=apoptosis-inducing factor, mitochondrion-associated, *Tnfrsf21*=tumor necrosis factor receptor superfamily, member 21. Triple-labeling identified **(B)** increased cleaved caspase 3**, (C)** increased cleaved caspase 9 and **(D)** unchanged cleaved caspase 8 in TH+ DRGN with vitE deficiency. Green: Th, Blue: DAPI nuclei. Red: **(B)** Cleaved caspase 3, **(C)** Cleaved caspase 9 and **(D)** cleaved caspase 8**.** White box inset magnified in last column. Fluorescent immunohistochemistry from 4 month WT, DEF, and SUPP mice. Scale bars= 10 μm (TH, Cleaved Cas3, Cas9, Cas 8 and merge) and 3 μm (enlarged; last column).

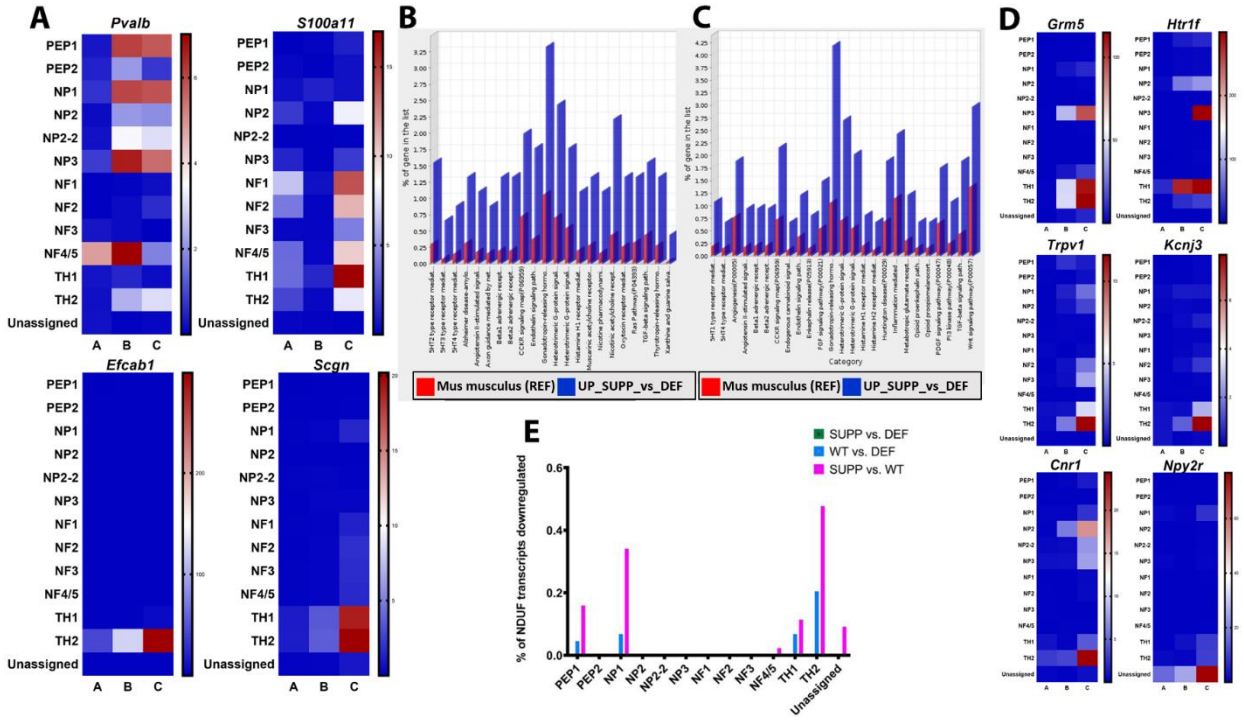

Figure S5, related to Fig. 1: Upregulation of Ca^{2+} binding transcripts and G-protein signaling pathways and downregulation of mitochondrial complex I transcripts in TH+ DRGNs with vitE deficiency. Heat maps, plotted by $-\log P_{adjusted}$, comparing the degree of upregulation for **(A)** selected Ca^{2+} binding transcripts in DRGN subpopulations with vitE deficiency. Representative Panther Pathway overrepresentation analysis (red=*Mus musculus* database, blue=overrepresented pathways of the SUPP vs WT groups) from the **(B)** TH1 and **(C)** TH2 subpopulations demonstrating upregulation of G-protein signaling pathways and G-protein coupled receptors (GPCRs). These pathways were identified as upregulated in 9/13 DRGN subpopulations (additional figures; **Figure S6**). **(D)** Heat maps, plotted by $-\log P_{adjusted}$, comparing the degree of upregulation for selected G-protein coupled receptor genes and the transient receptor potential vallinoid (*Trpv1*) channel in DRGN subpopulations with vitE deficiency. Contrast A= SUPP vs. WT, contrast B= WT vs. DEF , contrast C= SUPP vs. DEF. **(E)** Percent of mitochondrial complex I: NADH:ubiquinone oxidoreductase supernumerary subunits (NDUF) downregulated in DRGN subpopulations with α-TOH deficiency. The most pronounced downregulation was within the NP1 (34%) and TH2 (47%) subpopulations. *Cacna1e*= Cav2.3 intermediate voltage-activated Ca^{2+} channel, *Cnr1*=cannaboinoid receptor 1, *Efcab1*=EF-hand calcium binding domain 1, *Grm*=metabotropic glutamate receptor 5, *Hrt1f*=5HT receptor 1f, *Kcnj3*= GIRK1, *Kcnmb*=Potassium large conductance calcium-activated channel, subfamily M, beta, *Npy2r*=NPY receptor 2, *Pvalb*=parvalbumin, *S100a11*=S100 calcium-binding protein A11, *Scgn*=secretagogin.

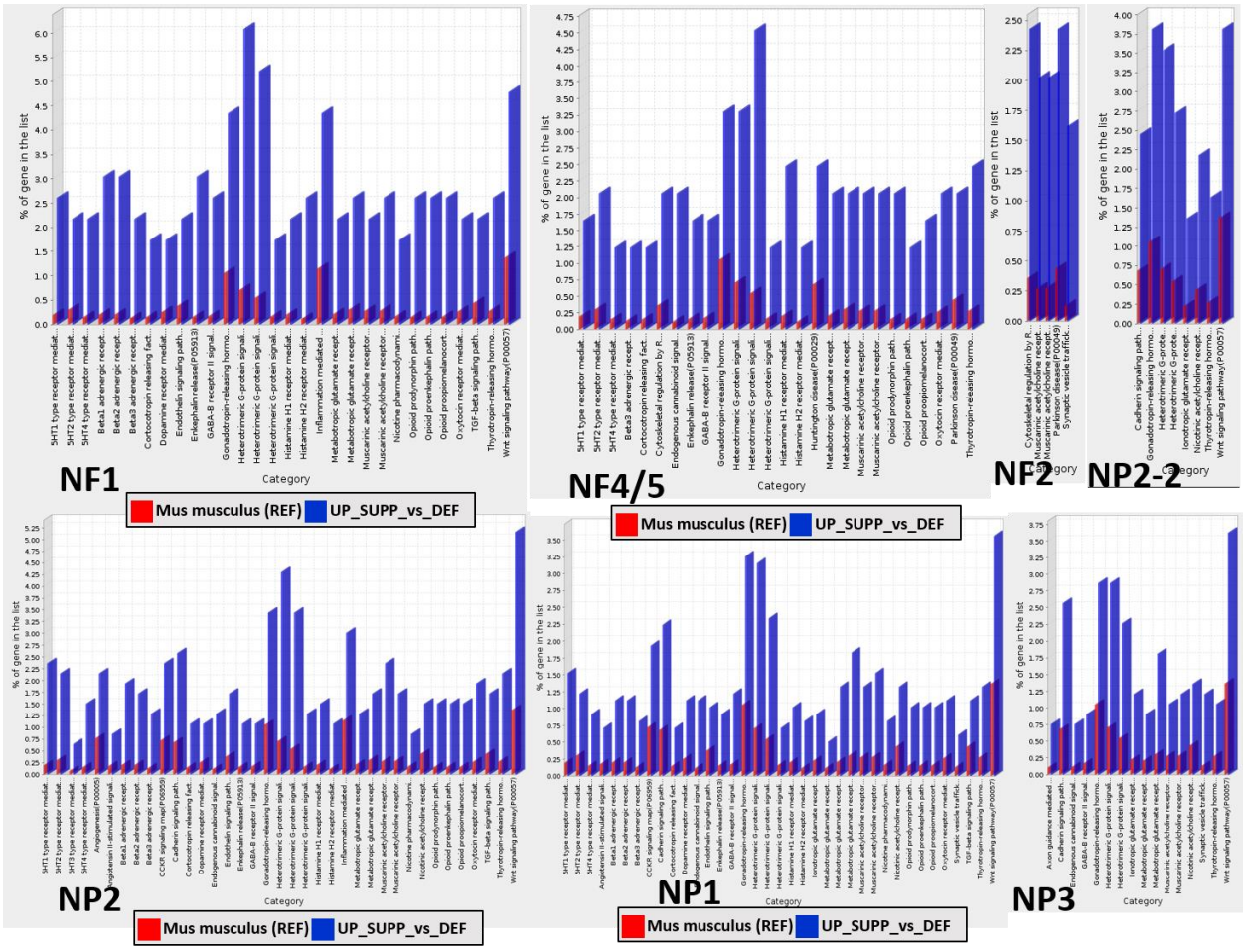

Figure S6, related to Fig. 1: Representative Panther Pathway overrepresentation analysis results of the SUPP vs DEF groups from the other DRG subpopulations, demonstrating upregulation of G-protein signaling pathways in a total of 9/13 DRG subpopulations (TH+ subpopulations in Figs 2D,E).

Supplemental Tables

Tables S1, S4 and S7 are separate Excel files due to size

Table S2, related to Fig. 1: Number/name of top genes defining each dorsal root ganglia (DRG) subpopulation			
DRG subpopulation	**# of genes defining each subpopulation**	**Median # of cells sequenced**	**Top transcripts defining neuronal subgroups**
PEP1 (peptidergic 1) Peptidergic nociception	139	1098	*Calca, Tac1, Kit, Ntrk1, Gal, Adcyap1, Gfra3*
PEP2 (peptidergic 2) Peptidergic nociception	82	141	*Ntrk1, Nefh, Cntnap2, Kit, Calca, Fam19a1*
NP1 Non-peptidergic nociception	92	465	*Mrgprd, Lpar3, Calca, Plxnc1, Scg3, Ctxn3, Gfra2*
NP2 Non-peptidergic nociception	63	102	*Mrgpra3, Ntrk1, Calca, Plxnc1, Adora2b, Cbln1*
NP2-2 Non-peptidergic nociception	25	169	*Crip1, Kcnmb1, Calca, Emp3*
NP3 Non-peptidergic nociception	187	328	*Osmr, Sst, Il31ra, Cysltr2, Nppb, Nts*
NF1 (neurofilament 1) Low threshold mechanoreceptors	72	113	*Necab2, Ntrk2, Cacna1h, Ldhb, Nefh, Htr1d*
NF2 (neurofilament 2) Low threshold mechanoreceptors	168	124	*Nefh, Ntrk2, Ntrk3, Calb1, Ldhb, Ret*
NF3 (neurofilament 3) Low threshold mechanoreceptors	59	96	*Nefh, Fam19a1, Ntrk3, Ldhb, S100b, Tuba4a*
NF4-5 (neurofilament 4-5) Proprioception	196	107	*Pvalb, Cntnap2, Spp1, Nefh, Cntnap2, Nxph1, Ldhb*
TH1 (tyrosine hydroxylase) Type C low-threshold mechanoreceptors	102	380	*Th, Piezo2, Slc17a8, Gfra2, Zfp521*
TH2 (tyrosine hydroxylase) Type C low-threshold mechanoreceptors	254	317	*Th, Piezo2, Slc17a8, Gfra2, Zfp521*
Unassigned	106	52	N/A

Table S3, related to Fig. 1: Number of differentially expressed transcripts (DETs) per DRG subpopulation within each contrast. Experimental groups defined in Transparent Methods										
		WT vs. DEF			SUPP vs. WT			SUPP vs. DEF		
Cluster#	ClusterName	#DETs	DOWNREGULATED (Panther)	UPREGULATED	#DETS	DOWNREGULATED (Panther)	UPREGULATED	#DETs	DOWNREGULATED	UPREGULATED
0.2	PEP1	228	62	166	65	14	51	465	143	322
1	NP1	463	78	385	154	56	98	1801	795	1006
3	TH1	249	33	216	95	33	62	520	64	456
4	NP3	391	75	316	92	35	57	787	113	674
5	TH2	398	77	321	122	59	63	1138	386	752
6	X	219	15	204	71	33	38	474	101	373
7	PEP2	66	11	55	21	2	19	186	34	152
8	NF2	53	10	43	48	12	36	495	231	264
9	NF4/5	54	3	51	43	9	34	343	88	255
10	NF1	114	14	100	59	12	47	314	63	251
11	NP2	273	7	266	110	42	68	535	62	473
12	NF3	88	15	72	52	7	45	333	107	226
13	Unassigned	192	22	170	100	13	87	424	44	380

Table S5, related to Fig. 2: Differentially expressed transcripts associated with Ca^{2+} and K^+ channels that passed $P_{FDR} < 0.05$ across the DRG subpopulations

		PEP1	PEP2	NP1	NP2	NP2-2	NP3	NF1	NF2	NF3	NF4/5	TH1	TH2	Un
Voltage-gated Ca^{2+} channels														
L-type ("Long-lasting")	*Cacna1c*								X			X	X	
P-type ("Purkinje")	*Cacna1a*													
N-type ("Neural"	*Cacna1b*			X										
R-type ("Residual")	*Cacna1e*			X	X	X	X	X		X	X	X	X	
Type-type ("Transient")	*Cacna1h*			X	X		X							
	Cacna1l	X		X	X	X	X		X					X
Ligand-gated Ca^{2+} channels														
IP_3 receptor	*Itpr1*													
	Itpr3													
Ryanodine receptor	*Ryr2*			X	X		X		X			X	X	
	Ryr3													
Two-pore channel	*Tpcn1*													
Cation channels of sperm	*Pkd2*													
Store-operated channels	*Orai1*													
	Orai2													
	Orai3													
K^+ channels														
Ca^{2+}-activated K^+ channels	*Kcnmb1*											X	X	
	Kcnmb2			X	X	X						X	X	
K^+ two-pore domain subfamily K	*Kcnk2*					X					X		X	
	Kcnk3			X	X							X	X	
	Kcnk12											X	X	
	Kcnk18	X	X									X	X	X
K^+ voltage-gated channel subfamily J (inward rectifying K^+ channels)	*Kncj2*			X	X	X		X				X	X	
	Kcnj3						X						X	
	Kcnj4	X		X	X		X							
K^+ voltage-gated channel	*Kcna2*			X		X	X							
	Kcnab1	X			X	X	X							
	Kcnb2											X	X	
	Kcnc1			X	X	X	X						X	
	Kcnc2			X	X	X			X	X	X			
	Kcnc4				X	X	X					X		
	Kcnd2		X	X		X	X							
	Kcnd3	X					X							
	Kcnh2			X	X		X							
	Kcnq2					X	X							
	Kcnq3	X		X			X							
	Kcnq5					X	X							
	Kcns1	X				X								X
	Kcns3										X	X	X	
	Kcnv1		X					X	X		X		X	X

Table S6, related to Fig. 1: Differentially expressed transcripts associated with synaptogeneis, axonal growth and myelination that passed $P_{FDR} < 0.05$ across the DRG subpopulations

		PEP1	PEP2	NP1	NP2	NP2-2	NP3	NF1	NF2	NF3	NF4/5	TH1	TH2	Un
Cerebellin precursor proteins synapse integrity and plasticity	*Cbln1*			X			X	X					X	
	Cbln2	X	X	X	X	X	X							
Sema domain– normal brain development, axon guidance and cell migration	*Sema4c*											X	X	
	Sema5a			X		X	X					X	X	
	Sema6a											X		
	Sema7a	X		X	X		X							
Solute carrier family 17 –uptake of glutamate at presynaptic nerve terminals	*Slc17a6*						X				X			
	Slc17a7	X		X										
	Slc17a8				X	X	X		X	X	X			
Unc-5 homology A – receptor for netrin required for axon guidance	*Unc5a*	X	X		X	X								
	Unc5b							X		X				X
	Unc5c						X					X	X	
	Unc5d			X		X				X		X	X	
	Unc13c							X					X	
Axonal growth and extension	*Bdnf* – neuronal survival and differentiation											X	X	
	Btbd3 – directs dendrites toward active axon terminals											X	X	
	Dpsyl2 - axonal guidance			X									X	
	Kif21a – kinesin family axonal transport			X									X	
	Ntrk1 – tyrosine kinase receptor involved in axonal extension			X				X	X		X	X	X	
	Rtn4r – axonal growth inhibition											X	X	
	Slit2 – axonal navigation	X		X	X	X	X			X			X	
Synaptic vesicle	*Cplx2* – complexin 2 formation of synaptic vesicle clustering			X									X	
	Stxbp6 – syntaxin binding protein	X		X	X	X	X						X	
	Sv2a – synaptic vesicle glycoprotein			X			X		X	X				
	Sv2b – synaptic vesicle glycoprotein			X	X							X	X	
	Syt3 – synaptotagmin III	X		X		X	X							
	Syt16 – synaptotagmin XVI			X		X		X					X	
	Sytl3 – synaptotagmin-like III						X	X				X	X	
Myelination	*Mbp* – myelin binding protein	X		X		X	X						X (Down)	
	Omg – Oligodendrocyte myelin glycoprotein			X	X	X						X	X	

Table S8, related to Fig. 1: Differentially expressed transcripts of the mitochondrial complex I:NADH:ubiquinone oxidoreductase supernumary subunits (NDUF)

	PEP1	PEP2	NP1	NP2	NP2-2	NP3	NF1	NF2	NF3	NF4/5	TH1	TH2	Un
Ndufa9			X									X	
Ndufa10			X										
Ndufa11	X		X									X	
Ndufa12			X									X	
Ndufa13													X
Ndufab1			X									X	
Ndufaf2												X	
Ndufaf3			X									X	
Ndufaf6			X										
Ndufaf7			X									X	
Ndufb2											X	X	
Ndufb3												X	
Ndufb4												X	
Ndufb6			X									X	
Ndufb8	X												
Ndufb9													X
Ndufb11	X												
Ndufc1	X											X	
Ndufs2			X									X	
Ndufs3												X	X
Ndufs4			X									X	
Ndufs5			X									X	
Ndufs6											X		
Ndufs7			X									X	
Ndufs8			X									X	
Ndufv1			X										
Ndufv3	X												

Transparent Methods

Contact for Reagent and Resource Sharing

Further information and requests for resources and reagents should be directed to and will be fulfilled by the Lead Contact, Carrie J. Finno (cjfinno@ucdavis.edu).

Reagents for scRNA-seq preparation

Growth medium for primary DRG cell culture consisted of five components that included: 500 mL nutrient mixture F-12 with phenol red stored at 4oC (Gibco™ Ham's F-12 Nutrient Mix), 5 mL Penicillin/Streptomycin stock (100 U/mL), 5 mL 100X N2 supplement, 10 mL 50X B-27 supplement, and 50 mL FBS (10% v/v). Stock solution (15% w/v) was prepared using 1.5 g of BSA (Sigma-Aldrich, St. Louis, MO) in 10 mL of F-12 medium. The same BSA lot number was used for WT, DEF and SUPP groups. The solution was placed in a 37°C water bath to dissolve BSA further. The F-12 medium was filter-sterilized (using a 40µm Flowmi™ Cell Strainer) and made into a final solution using a 12 mL syringe/filter. The solution was made the day of DRG cell processing. Stock solution (12.5 mg/mL; 1.25% w/v) was prepared by placing 50 mg collagenase IV in 4 mL F-12 (no phenol red) and was sterilized by a 0.22 µm filter. When resecting the DRG cells, 200 µL of collagenase IV (Gibco™ 17104019) was added to 1.8 mL HBSS (Hank's Balanced Salt Solution).

Experimental model and subject details

Mice

Animals were housed and cared for under the University of California Davis (UCD) and University of Reno (UNR) standing committee on animal use and care (IACUC) as well as the Guide for the Care and Use of Laboratory animals (8th edition, 2011). All procedures performed were also approved by the University (UCD and UNR) IACUC. A rederived colony of mixed (50% C57BL6 and 50% 129/SvJae) mice heterozygous for the deletion (*Ttpa*$^{+/-}$) were crossed with C57BL6/J (*Ttpa*$^{-/-}$) mice to establish a colony of *Ttpa*$^{-/-}$ mice. Offspring were genotyped using specific primers for *Ttpa*, and genotypes confirmed by western blot analysis of hepatic TTP using an anti-TTP antibody as previously described (Terasawa et al., 2000).

At weaning, *Ttpa*$^{+/+}$ mice were fed a normal diet (35 mg of dl-α-tocopheryl acetate/kg, vitE+; WT) while *Ttpa*$^{-/-}$ mice were fed either an α-TOH-deficient diet (<10 mg of dl-α-tocopheryl acetate/kg, vitE-; DEF), or α-TOH-supplemented diet (600 mg of dl-α-tocopheryl acetate/kg, vitE+++; SUPP) diet. Custom Teklad non-irradiated vacuum-packaged diets were ordered through Harlan Laboratories (Madison, WI) and were identical to those previously used in this mouse model (Finno et al., 2018, Ulatowski et al., 2014). To prevent oxidation, diets were maintained at -20°C and used within six months. Mouse diets were replaced once per week, and high-performance liquid chromatography with fluorescence detection used to confirm dietary α-TOH concentrations was performed as previously described (Finno et al., 2018).

Method Details

Neurobehavioral assessment

Examination of mechanical sensation was performed on mice at 6 months of age, when the onset of ataxia are first noticeable (Finno et al., 2018). Mice were housed under conditions of

constant temperature (20°C), light (6:00 am to 6:00 pm), and with access to food and water ad libitum. Testing apparatus was cleaned with 70% ethanol to remove animal odors before and after each test. Experiments were performed with 8-15 mice per group, consisting of ~50% male and 50% female. Each test was performed at one time point, 1-2 days before sacrifice. The von Frey filament assay was performed as previously described (Martinov et al., 2013). Mice were habituated to the experimental environment for at least 30 minutes. Briefly, von Frey filaments of increasing stiffness (0.008-1.4g) were applied on both hind paws planter surface with enough pressure to bend the filament, to determine the stimulus intensity threshold stiffness required to elicit a paw withdrawal response. A total of six recordings were performed per mouse (initial reflex, followed by five "up-down" stimuli). Dixon's score was calculated as previously described (Dixon, 1965).

Dorsal root ganglion neuron (DRGN) isolation

At 5-6 months of age, one male and one female mouse were sacrificed with pentobarbital (>100 mg/kg IP). After euthanasia, the spinal column was removed by making lateral incisions on both sides. The spinal cord was then severed at the C1 (cervical) and L6 (lumbar) vertebrae. The dorsal portion of the spinal column was removed, exposing the spinal cord. Shortly after, the spinal cord was removed to expose the DRG. Dorsal root ganglia were extracted using micro dissecting forceps and microscissors. Dorsal root ganglia were placed in a petri-dish containing 1.8 mL of ice-cold HBSS. The spines of the dorsal root ganglia were trimmed using microdissection scissors.

Following DRG removal, 200 µL of collagenase was added to the HBSS solution containing the DRG. The whole DRG were placed in an incubator for 2 hours at 37^{o}C, 5% CO_2. The DRG were subsequently transferred to a 15 ml conical centrifuge tube and washed twice with 10 mL of pre-warmed growth medium to remove any remaining collagenase solution. Collagenase is inhibited by cysteine, which is a component of the F-12 nutrient mix. The 570 mL stock solution of growth medium contained 500 mL F-12, 5 mL Pen/Strep, 5 mL 100X N2 supplement, 10 mL 50X B27 supplement, and 50 mL FBS. While in the 15 mL conical tube, DRG were triturated to dissociate the DRG into individual cells. Afterward, the volume was aspirated and filtered through a 40-µm FlowmiTM Cell Strainer. The cell suspension was slowly dripped onto 10 mL 15% BSA (bovine serum albumin), pre-warmed growth medium in a 15 mL conical tube and centrifuged at 200 x g for 20 minutes. The BSA stock solution contained 1.5 g of BSA dissolved in 10 mL of F-12. The supernatant was aspirated, leaving approximately 20 µL covering the cell pellet. In this protocol, nerve growth factor (NGF) was not used in the growth medium as NGF alters gene expression (Lindsay and Harmar, 1989).

Cell count/viability and RNA quality assurance

A hemocytometer was used to determine the viability of the cells stained with trypan blue. Once non-neuronal cells were removed using a 10 mL 15% BSA treatment and centrifuged at 200 x g, a portion of the cell suspension was aliquoted into a 0.5 mL microcentrifuge tube. Despite this treatment, some non-neuronal cells may survive the removal process. Depending on the volume of the cell suspension, a 1:1 mixture was made using 0.4% trypan blue solution. The mixture was pipetted into the V-shaped groove of the coverslip. The viable and non-viable cells in each of the four corner quadrants were multiplied by 104. To obtain the percentage of viable

cells, the following formula was used: % viable cells= [1.00 - (# of nonviable cell / # of total cells)] x 100. Samples were analyzed on an Agilent Bioanalyzer before and after library preparation to ensure quality RNA and cDNA was sequenced.

Single-cell RNA-sequencing

Barcoded 3' single-cell libraries were prepared from single-cell suspensions using the Chromium Single Cell 3' Library and Gel b ead kit v2 (10X Genomics, Pleasanton, California). Libraries were pooled and sequenced on an Illumina HiSeq4000 with pair-end 100 bp reads. Cellranger v.2.0.1 and bcl2fastq v.2.17.1.14 commands mkfastq and count were used to generate fastq files per sample, align to mm10, filter, and perform barcode and UMI counting. Analyses were conducted in R, version 3.4.4 (Team, 2018). Normalization, clustering, and calculation of TSNE (van der Maaten and Hinton, 2008) coordinates were conducted using Seurat, version 2.3.0 (Satija et al., 2018). Differential expression analyses between treatments, adjusting for sample and sex, were conducted on the filtered and normalized data using limma, version 3.32.10 (Ritchie et al., 2015). Pathway analyses were performed using Panther Pathway overrepresentation analysis (http://pantherdb.org/).

Single-molecule fluorescence in situ hybridization (smFISH) with RNAscope

Mice were anesthetized with an intraperitoneal injection of ketamine (100 mg/kg) and xylazine (10 mg/kg), and were transcardially perfused with diethyl-pyrocarbonate (DEPC)-treated phosphate buffer saline (PBS) and 4% paraformaldehyde (PFA) to preserve RNA. Dorsal root ganglia (DRG) were extracted using micro dissecting forceps and micro-scissors. Dorsal

root ganglia were placed in a petri-dish containing 1.8 mL of ice-cold DEPC-treated PBS. The tissues were trimmed using a surgical scalpel blade and were kept in a 4% PFA in DEPC-treated solution, overnight on a shaker at 4°C. Samples were sequentially dehydrated in 10%, 20%, and 30% sucrose solution at 4°C for 1 hr, 2 hr, and overnight, respectively. Samples were transferred into optimal cutting temperature (OCT) compound for a minimum of 1 hr at 4°C and then snap frozen, using a dry ice-ethanol mixture. Samples were cryo-sectioned to a thickness of 14 μm, placed onto Superfrost slides and stored at -80°C until processed.

Probe hybridization and immunofluorescent staining

Probe hybridization was performed according to the manufacturer's instructions (Advanced Cell Diagnostics, ACD). Sections were immersed in pre-chilled 4% PFA for 15 min at 4°C. Sections were then dehydrated at room temperature (RT) in 50%, 70% and twice in 100% ethanol for 5 min each and allowed to dry for 1-2 min. Fixation and dehydration were followed by hydrogen peroxide reaction for 10 min at RT then, protease digestion, using protease 4 for 30 min at RT. Slides were incubated with probes in 2 hours at 40°C. To amplify and detect signals, sections were treated as follows at 40°C: AMP1 for 30 min, followed by AMP2 for 30 min, AMP3 for 15 min, the appropriate HRP channel for 15 min, Opal dye for 30 min, and HRP blocker for 15 min. Each of these alternated with a washing step two times for 2 min at RT. Probes for *Kcnmb2, Kcnq3, Kcnv1* and *Cacna1e* and controls were obtained from ACD. Sequences of the target probes and label probe are proprietary. Detailed information about the probe sequences can be obtained by signing a non-disclosure agreement provided by the manufacturer.

For subsequent immunofluorescent staining, slides were treated with 10% blocking solution for 30 min at RT, incubated with primary antibody (Tyrosine Hydroxylase, LSbio, 1:500 dilution), overnight at 4°C, washed with TBS-0.005%Tween20 three times for 5 min each, incubated with secondary antibody (Alexa 647, Life Technologies, 1:500) for 2 hours at RT, and again washed with TBS-0-005% Tween20 three times for 5 min each. Incubation in DAPI solution for 30s at RT was performed to label cell nuclei. Slides were then mounted in Fluoromount-G and sealed under a coverslip.

Immunofluorescence

Following microdissection, the tissue was fixed at 4°C in 4% PFA in PBS and 10% and 30% sucrose at 4°C overnight, then embedded in OCT for cryo-sectioning in the cryo-mold. Sections of 10-µm were washed in PBS, permeabilized in 0.1% Triton X-100 for 10 min, and then incubated for 60 min in a blocking solution containing 10% goat serum. The sections were incubated with primary antibody overnight at 4°C in a humid-chamber. The rinsed sections were then incubated (2 hrs; RT) in a fluorescent dye-conjugated secondary antibody. The following primary antibodies were used: rabbit anti KCNQ3 (Abcam, #ab16228), rabbit anti KCNV1 (Abcam, #ab175548), mouse anti KCNMB2 (Abcam, #ab94598), rabbit anti $Ca_v2.3$ (Alomone Labs, #ACC-006), mouse anti tyrosine hydroxylase (TH; LSBio, #LS-C338121), rabbit anti TH (LSBio, #LS-C354112), rabbit anti cleaved caspase-3, -8 and -9 (Cell Signaling Technology, #9664, #8592, and #9509), rabbit anti total caspase-3 and -9 (Abcam, #ab13847, and #ab202068). Secondary antibodies were Alexa 488-conjugated affinity-purified goat anti-rabbit IgG, Alexa 488-conjugated affinity-purified goat anti-mouse IgG, Cy3-conjugated affinity-

purified goat anti-rabbit IgG, Alexa 555-conjugated affinity-purified goat anti-mouse IgG (Invitrogen and Jackson Labs). Images were captured with a Nikon A1 confocal microscope.

Isolation of DRGNs for electrophysiological recordings

Dorsal root ganglion neurons (DRGNs) were isolated from male and female mice from each experimental group. Dissected tissue was removed and placed in a solution containing Minimum Essential Medium with Hank's salt (Invitrogen), 0.2 g/L kynurenic acid, 10 mM $MgCl_2$, 2% fetal bovine serum (FBS; v/v), and 6 g/L glucose. Tissues were digested in an enzyme mixture containing collagenase type I (1 mg/mL) and DNase (1 mg/mL) at 37 °C for 20 min. After a series of gentle trituration and centrifugation in 0.45 M sucrose, the cell pellets were reconstituted in 900 mL culture media (Neurobasal-A, supplemented with 2% B27 (v/v), 0.5 mM L-glutamine, 100 U/mL penicillin; Invitrogen) and filtered through a 50-μm cell strainer for cell culture. DRGNs were cultured for 24 to 48 hrs. All electrophysiological experiments were performed at RT (21-22°C). Reagents were obtained from Sigma-Aldrich (St. Louis, MO) unless otherwise noted. A stock solution of rSNX-482 was made and (10 mM) stored at -20^{o}C.

To identify mechanosensitive DRGNs, small-diameter neurons were identified, and mechanical stimulation was achieved using a fire-polished and sylgard-coated glass pipette (tip diameter ~1-2 μm), positioned at an angle of ~60° to the DRGN being recorded. Downward movement of the probe toward the cell was driven by a piezo-electric crystal micro stage (E660 LVPZT Controller/Amplifier; Physik Instruments). The probe was typically positioned close to the cell body without any visible membrane deformation. We assessed for mechanical sensitivity using a series of mechanical steps in ~0.42 μm increments applied every 10 to 20 s, which allowed

for the full recovery of mechanosensitive currents between steps. Inward mechanically-activated (MA) currents were recorded at a holding potential of -70 mV. For voltage-clamp recordings of MA currents, patch pipettes had resistance of 2-3 MΩ when filled with an internal solution consisting of (in mM): 70 CsCl, 55 NMDGCl, 10 HEPES, 10 EGTA, 1 $CaCl_2$, 1 $MgCl_2$, 5 MgATP, and 0.5 Na_2GTP (pH adjusted to 7.3 with CsOH). The extracellular solution consisted of (in mM): 130 NaCl, 3 KCl, 1 $MgCl_2$, 10 HEPES, 2.5 $CaCl_2$, 10 glucose and 2 CsCl (pH was adjusted to 7.3 using NaOH).

Data analyses were performed using pClamp8 (Axon Instruments) and Origin software (Microcal Software, Northampton, MA) offline. The peak mechanically-activated (MA) current (I_{MA}) for each step displacement $I(X)$ was expressed in the form of the probability of channel opening (P_o of I/I_{max}) with a Boltzmann equation $P_o = 1/[1 + e^{z(X - X_{1/2})/(kT)}]$ to obtain single-channel gating force, z, and the displacement at 50% open probability ($X_{1/2}$), and T is temperature.

Current-clamp experiments

Whole-cell membrane potential recordings were performed using an Axopatch 200B amplifier (Molecular Devices, San Jose, CA). Membrane potentials were amplified, bandpass filtered (2-10 kHz), and digitized at 5-50 kHz using an analog-to-digital converter (Digidata 1200, Molecular Devices) as described earlier (Levic et al., 2007, Rodriguez-Contreras et al., 2008). Electrodes (2-3 MΩ) were pulled from borosilicate glass pipettes, and the tips were fire-polished. Extracellular/bath solution consisted of (in mM) 145 NaCl, 6 KCl, 1 $MgCl_2$, 2 $CaCl_2$, 10 D-glucose, and 10 4-(2-hydroxyethyl)-1-piperazineethanesulfonic acid (HEPES), pH 7.3. The

normal pipette/internal solution contained (in mM) 146 KCl, 1 $MgCl_2$, 0.1 $CaCl_2$, 5 ethylene glycol-bis(β-aminoethyl ether)-N,N,N′,N′-tetraacetic acid (EGTA) 4 MgATP, 0.4 NaGTP and 10 HEPES, pH 7.3. The seal resistance was typically 5-10 GΩ. Data analyses were performed using the pClamp and Origin software (MicroCal Inc., Northampton, MA). Where appropriate, pooled data are presented as means $\pm$ S.E.

Voltage-clamp experiments

Whole-cell voltage-clamp recordings were conducted at room temperature (RT) using an Axopatch 200B amplifier and filtered at 2kHz through a low-pass Bessel filter. Data were digitized at 0.5-1.0 kHz using a Digi-Data analog-to-digital converter. To study Ca^{2+} currents in DRGNs, after ~2 days in culture, the cells were held in a bath solution (in mM; 60 NMGCl, 50 CholineCl, 10 NaCl, 20 tetraethylammonium chloride (TEACl), 5 4-Aminopyridine (4-AP), CsCl, 5 $CaCl_2$, 0.5 $MgCl_2$, 10 HEPES and 5 Glucose at pH 7.4). Freshly reconstituted tetrodotoxin (TTX) (final concentration, 2 μM) was added to the bath solution to further suppression Na^+ currents. The internal solution contained (in mM) 60 Cs-gluconate, 60 mM N-methyl-d-glucamine (NMDG)-Cl, 2 $MgCl_2$, 0.1 $CaCl_2$, 5 K_2ATP, 0.5 GTP-sodium, 5 EGTA, and 10 HEPES, pH 7.35, with CsOH.

K^+ currents were measured using bath solution containing (in mM: 60 NMGCl, 35 CholineCl, 5 KCl, 10 NaCl, 0.05 $CaCl_2$, 0.5 $MgCl_2$, 10 HEPES and 5 glucose at pH 7.4). Freshly reconstituted tetrodotoxin (TTX) (final concentration, 2 μM) was added to the bath solution to suppression Na^+ currents. The pipette solution contained (in mM; 140 KCl, 1 $MgCl_2$, 10 HEPES, 2.5 EGTA, 1 $CaCl_2$, and 4 MgATP, at pH 7.2). Freshly reconstituted tetrodotoxin (TTX) (final concentration, 2 μM) was added to the external solution to suppression Na^+ current when

measuring K^+ and Ca^{2+} currents. Ca^{2+} currents were also suppressed, but not eliminated using 50 μM external Ca^{2+}

Borosilicate glass pipettes were pulled using a Sutter P-97 Flaming Brown Micropipette Puller (Sutter Instruments) and fire-polished for an optimal pipette resistance (2-3 MΩ). Access resistance was compensated further by at least 80%. After achieving a GΩ-seal, gentle suction was applied to form a whole-cell configuration. In all cases, liquid junction potentials were measured and corrected as described previously (Rodriguez-Contreras and Yamoah, 2001). Currents were activated with depolarizing voltage steps from -120 to 40 mV, using a ΔV of 10 mV and holding potentials at -40, -60 and -90 mV. All protocols were employed without online leak subtraction.

Quantification and Statistical Analysis

Statistical analysis

All data was evaluated for normality using a Shapiro-Wilk test. Parametric data were analyzed via a one-way ANOVA compared the three genotype / diet groups followed by a Tukey post-hoc test. Non-parametric data were analyzed with a Kruskal-Wallis test followed by Dunn's multiple comparison tests. For quantification of mRNA via RNA-scope, four high-power fields were evaluated from n=2-3 mice in each group and number of mRNA TH+ DRGNs quantified. For electrophysiologic recordings, n=2-3 pooled mice with 9-15 DRGNs per experimental group were recorded. Significance was set at $p < 0.05$.

Data and Software Availability

The raw and processed data for scRNA-seq individual libraries have been deposited in the NCBI Gene Expression Omnibus (GEO) under ID codes (GEO:GSE128276, GSM3670444, GSM3670445, GSM3670446, GSM3670447, GSM3670448, GSM3670449).

Supplemental References

DIXON, W. J. 1965. The Up-and-Down Method for Small Samples. *J Am Statist Assoc* 60**,** 967-978.

FINNO, C. J., BORDBARI, M. H., GIANINO, G., MING-WHITFIELD, B., BURNS, E., MERKEL, J., BRITTON, M., DURBIN-JOHNSON, B., SLOMA, E. A., MCMACKIN, M., CORTOPASSI, G., RIVAS, V., BARRO, M., TRAN, C. K., GENNITY, I., HABIB, H., XU, L., PUSCHNER, B. & MILLER, A. D. 2018. An innate immune response and altered nuclear receptor activation defines the spinal cord transcriptome during alpha-tocopherol deficiency in Ttpa-null mice. *Free Radic Biol Med,* 120**,** 289-302.

LEVIC, S., NIE, L., TUTEJA, D., HARVEY, M., SOKOLOWSKI, B. H. & YAMOAH, E. N. 2007. Development and regeneration of hair cells share common functional features. *Proc Natl Acad Sci U S A,* 104**,** 19108-13.

LINDSAY, R. M. & HARMAR, A. J. 1989. Nerve growth factor regulates expression of neuropeptide genes in adult sensory neurons. *Nature,* 337**,** 362-4.

MARTINOV, T., MACK, M., SYKES, A. & CHATTERJEA, D. 2013. Measuring changes in tactile sensitivity in the hind paw of mice using an electronic von Frey apparatus. *J Vis Exp***,** e51212.

RITCHIE, M. E., PHIPSON, B., WU, D., HU, Y., LAW, C. W., SHI, W. & SMYTH, G. K. 2015. limma powers differential expression analyses for RNA-sequencing and microarray studies. *Nucleic Acids Res,* 43**,** e47.

RODRIGUEZ-CONTRERAS, A., LV, P., ZHU, J., KIM, H. J. & YAMOAH, E. N. 2008. Effects of strontium on the permeation and gating phenotype of calcium channels in hair cells. *J Neurophysiol,* 100**,** 2115-24.

SATIJA, R., BUTLER, A. & HOFFMAN, P. 2018. Seurat: Tools for Single Cell Genomics. R package version 2.3.0.

TEAM, R. C. 2018. R: A language and environment for statistical computing. R Foundation for Stati stical Computing. Vienna, Austria.

TERASAWA, Y., LADHA, Z., LEONARD, S. W., MORROW, J. D., NEWLAND, D., SANAN, D., PACKER, L., TRABER, M. G. & FARESE, R. V., JR. 2000. Increased atherosclerosis in hyperlipidemic mice deficient in alpha -tocopherol transfer protein and vitamin E. *Proc Natl Acad Sci U S A,* 97**,** 13830-4.

ULATOWSKI, L., PARKER, R., WARRIER, G., SULTANA, R., BUTTERFIELD, D. A. & MANOR, D. 2014. Vitamin E is essential for Purkinje neuron integrity. *Neuroscience,* 260**,** 120-9.

VAN DER MAATEN, L. J. P. & HINTON, G. E. 2008. Visualizing High-Dimensional Data Using t-SNE. *J of Machine Learning Res,* 9**,** 2579-2605.